frontiers

Mass and energy balance calculations for an artificial ice reservoir (Icestupa)

Suryanarayanan Balasubramanian [1,*], **Martin Hoelzle** [1], **Michael Lehning** [2], **Sonam Wangchuk** [3], **Johannes Oerlemans** [4] **and Felix Keller** [5]

[1] *University of Fribourg, Fribourg, Switzerland*
[2] *WSL Institute for Snow and Avalanche Research, Davos, Switzerland*
[3] *Himalayan Institute of Alternatives Ladakh, Leh, India*
[4] *Institute for Marine and Atmospheric Research, Utrecht University, Utrecht, The Netherlands*
[5] *Academia Engiadina, Samedan, Switzerland*

Correspondence*:
Suryanarayanan Balasubramanian
suryanarayanan.balasubramanian@unifr.ch

1 MODEL SETUP

A bulk energy and mass balance model is used to calculate the amounts of ice, meltwater, water vapour and runoff water of the AIR every hour. This model consists of four modules which calculate its, a) geometric evolution , b) energy balance, c) surface temperature and d) mass balance as shown schematically in Fig. **??**.

1.1 Geometric evolution

Radius r^i_{ice} and height h^i_{ice} define the dimensions of the Icestupa assuming its geometry to be a cone as shown in Fig. 1. The surface area A^i exposed to the atmosphere and volume V^i are:

$$A = \pi \cdot r_{ice} \cdot \sqrt{{r_{ice}}^2 + {h_{ice}}^2} \tag{1}$$

$$V = \pi/3 \cdot {r_{ice}}^2 \cdot h_{ice} \tag{2}$$

Note that we do not specify the time step superscript i of the shape variables A, V, r_{ice} and h_{ice} for brevity. The equations used henceforth display model time step superscript i only if it is different from the current time step.

With the mass of the Icestupa M_{ice}, its current volume can also be expressed as:

$$V = M_{ice}/\rho_{ice} \tag{3}$$

where ρ_{ice} is the density of ice (917 $kg\,m^{-3}$). The model of the Icestupa is initialised with a thickness of Δx (defined in 1.2) and a circular area of radius r_F. The constant r_F represents the mean spray radius of the fountain. This fountain spray radius is determined by

During subsequent time steps, the dimensions of the Icestupa evolve assuming a uniform ice formation and decay across its surface area with an invariant slope $s_{cone} = \frac{h_{ice}}{r_{ice}}$ as shown in Fig. 1. During these time

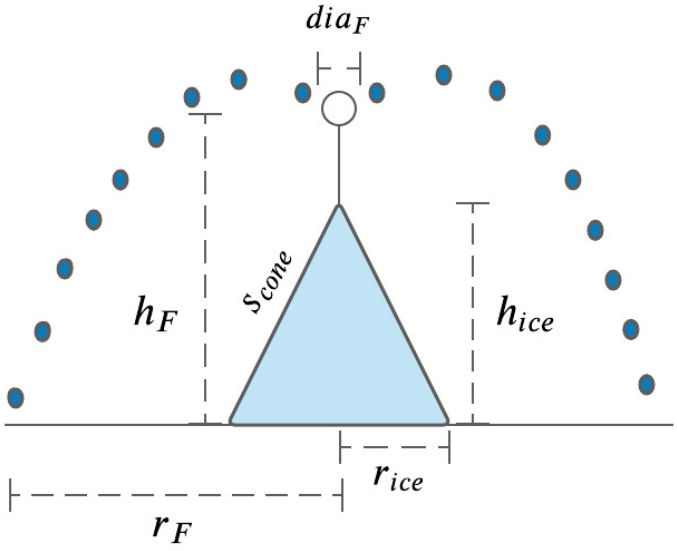

Figure 1. Shape variables and fountain constants of the EP Icestupa. r_{ice} is the radius, h_{ice} is the height and s_{cone} is the slope of the ice cone. r_F is the spray radius, h_F is the height and dia_F is the nozzle diameter of the fountain.

steps, the volume is parameterised using Eqn. 2 as:

$$V = \pi/3 \cdot {r_{ice}}^3 \cdot s_{cone} \tag{4}$$

However, the Icestupa cannot outgrow the maximum range of the water droplets ($(r_{ice})_{max} = r_F$). Combining equations 2, 3 and 4, the geometric evolution of the Icestupa at each time step i can be determined by considering the following rules:

$$(r_{ice},\, h_{ice}) = \begin{cases} (r_F,\, \Delta x) & \textit{if } i = 0 \\ (r_{ice}^{i-1},\, \frac{3 \cdot M_{ice}}{\pi \cdot \rho_{ice} \cdot (r_{ice}^{i-1})^2}) & \textit{if } r_{ice}^{i-1} \geq r_F \textit{ and } \Delta M_{ice} > 0 \textit{ where } \Delta M_{ice} = M_{ice}^{i-1} - M_{ice}^{i-2} \\ (\frac{3 \cdot M_{ice}}{\pi \cdot \rho_{ice} \cdot s_{cone}})^{1/3} \cdot (1,\, s_{cone}) & otherwise \end{cases} \tag{5}$$

1.2 Energy Balance

The energy balance equation (Hock, 2005) for the Icestupa is formulated as follows:

$$q_{SW} + q_{LW} + q_L + q_S + q_F + q_G = q_{surf} \tag{6}$$

where q_{surf} is the surface energy flux in $[W\, m^{-2}]$; q_{SW} is the surf shortwave radiation; q_{LW} is the surf longwave radiation; q_L and q_S are the turbulent latent and sensible heat fluxes. q_F represents the heat exchange of the fountain water droplets with the AIR ice surface. q_G represents ground heat flux between Icestupa surface and Icestupa interior. Energy transferred in the direction of the ice surface is always denoted as positive and away as negative.

Equation 6 is usually referred to as the energy budget for "the surface", but practically it must apply to a surface layer of ice with a finite thickness Δx. The energy flux acts upon the Icestupa surface layer

which has an upper and a lower boundary defined by the atmosphere and the ice body of the Icestupa, respectively. The parameter selection for Δx is based on the following two arguments: (a) the ice thickness Δx should be small enough to represent the surface temperature variations every model time step Δt and (b) Δx should be large enough for these temperature variations to not reach the bottom of the surface layer. Therefore, we introduced a 20 mm thick surface layer for a model time step of 1 hour, over which the energy balance is calculated. A sensitivity analysis was later performed to understand the influence of this factor. Here, we define the surface temperature T_{ice} to be the modelled average temperature of the Icestupa surface layer and the energy flux q_{surf} is assumed to act uniformly across the Icestupa area A.

1.2.1 Net Shortwave Radiation q_{SW}

The surf shortwave radiation q_{SW} is computed as follows:

$$q_{SW} = (1 - \alpha) \cdot (SW_{direct} \cdot f_{cone} + SW_{diffuse}) \tag{7}$$

where SW_{direct} and $SW_{diffuse}$ are the ERA5 direct and diffuse short wave radiation, α is the modelled albedo and f_{cone} is the area fraction of the ice structure exposed to the direct shortwave radiation.

We model the albedo using a scheme described in Oerlemans and Knap (1998). The scheme records the decay of albedo with time after fresh snow is deposited on the surface. δt records the number of time steps after the last snowfall event. After snowfall, albedo changes over a time step, δt , as

$$\alpha = \alpha_{ice} + (\alpha_{snow} - \alpha_{ice}) \cdot e^{(-\delta t)/\tau} \tag{8}$$

where α_{ice} is the bare ice albedo value (0.35), α_{snow} is the snow ice albedo value (0.85) and τ is a decay rate, which determines how fast the albedo of the ageing snow reaches this value. The decay rate τ is assumed to have a base value of 10 days similar to values obtained by Schmidt et al. (2017) for wet surfaces and its maximal value is set based on observations by Oerlemans and Knap (1998) as shown in Table 1. Furthermore, the albedo α varies depending on the water source that formed the current Icestupa surface. Correspondingly, the albedo is reset to the value of bare ice albedo if the fountain is spraying water onto the current ice surface and to the value of fresh snow albedo if a snowfall event occurred. Snowfall events are assumed if the air temperature is below $T_{ppt} = 1°C$ (Fujita and Ageta, 2000).

The area fraction f_{cone} of the ice structure exposed to the direct shortwave radiation depends on the shape considered. The direct solar radiation incident on the AIR surface is first decomposed into horizontal and vertical components using the solar elevation angle θ_{sun}. For a conical shape, half of the total curved surface is exposed to the vertical component of the direct shortwave radiation and the projected triangle of the curved surface is exposed to the horizontal component of the direct shortwave radiation. The solar elevation angle θ_{sun} used is modelled using the parametrisation proposed by Woolf (1968). Accordingly, f_{cone} is determined as follows:

$$f_{cone} = \frac{(0.5 \cdot r_{ice} \cdot h_{ice}) \cdot cos\theta_{sun} + (\pi \cdot {r_{ice}}^2/2) \cdot sin\theta_{sun}}{\pi \cdot r_{ice} \cdot ({r_{ice}}^2 + {h_{ice}}^2)^{1/2}} \tag{9}$$

The ERA5 diffuse shortwave radiation is assumed to impact the conical Icestupa surface uniformly.

1.2.2 Net Longwave Radiation q_{LW}

The surf longwave radiation q_{LW}, for which there were no direct measurements available at EP, is determined as follows:

$$q_{LW} = LW_{in} - \sigma \cdot \epsilon_{ice} \cdot (T_{ice} + 273.15)^4 \tag{10}$$

where T_a represents the measured air temperature, T_{ice} is the modelled surface temperature, both temperatures are given in [$^\circ C$], $\sigma = 5.67 \cdot 10^{-8}\, Jm^{-2}s^{-1}K^{-4}$ is the Stefan-Boltzmann constant, LW_{in} denotes the incoming longwave radiation derived from the ERA5 dataset and ϵ_{ice} is the corresponding emissivity value for the Icestupa surface (see Table 1).

1.2.3 Turbulent sensible q_S and latent q_L heat fluxes

The turbulent sensible q_S and latent heat q_L fluxes are computed with the following expressions proposed by Garratt (1992):

$$q_S = c_a \cdot \rho_a \cdot p_a / p_{0,a} \cdot \frac{\kappa^2 \cdot v_a \cdot (T_a - T_{ice})}{\left(\ln \frac{h_{AWS}}{z_{ice}}\right)^2} \tag{11}$$

$$q_L = 0.623 \cdot L_s \cdot \rho_a / p_{0,a} \cdot \frac{\kappa^2 \cdot v_a (p_{v,a} - p_{v,ice})}{\left(\ln \frac{h_{AWS}}{z_{ice}}\right)^2} \tag{12}$$

where h_{AWS} is the measurement height above the ground surface of the AWS (in m), v_a is the wind speed in [$m\, s^{-1}$] and M_F denotes fountain water spray mass in [kg]. c_a is the specific heat of air at constant pressure (1010 J $kg^{-1}K^{-1}$), ρ_a is the air density at standard sea level (1.29 kgm^{-3}), $p_{0,a}$ is the air pressure at standard sea level (1013 hPa), κ is the von Karman constant (0.4), L_s is the heat of sublimation (2848 $kJ\, kg^{-1}$) and z_{ice} (1.7 mm) denotes the roughness length of ice (momentum and scalar). The vapor pressures over air ($p_{v,a}$) and ice ($p_{v,ice}$) was obtained using the following formulation given in WMO (2018):

$$\begin{aligned} p_{v,a} &= 6.107 \cdot 10^{(7.5 \cdot T_a / (T_a + 237.3))} \\ p_{v,ice} &= (1.0016 + 3.15 \cdot 10^{-6} \cdot p_a - 0.074 \cdot p_a^{-1}) \cdot (6.112 \cdot e^{(22.46 \cdot T_{ice} / (T_{ice} + 272.62))}) \end{aligned} \tag{13}$$

where p_a is the measured air pressure in [hPa].

1.2.4 Fountain water heat flux q_F

The total energy flux is further influenced through the heat flux caused by the water that was additionally added to the surface of the Icestupa during the time the fountain was running. We take this interaction between the fountain water and the ice surface into account by assuming that the ice surface temperature remains constant at 0 $^\circ C$ during time steps when the fountain is active. This process can be divided into two simultaneous steps: (a) the water temperature T_{water} is cooled to 0 $^\circ C$ and (b) the ice surface temperature is warmed to 0 $^\circ C$. Process (a) transfers the necessary energy for process (b) throughout the fountain runtime. We further assume that this process is instantaneous, i.e. the ice temperature is immediately set to 0 $^\circ C$ within just one time step Δt when the fountain is switched on. Thus, the heat flux caused by the fountain water is calculated as follows:

$$q_F = \begin{cases} 0 & \textit{if } \Delta M_F = 0 \\ \frac{\Delta M_F \cdot c_{water} \cdot T_{water}}{\Delta t \cdot A} + \frac{\rho_{ice} \cdot \Delta x \cdot c_{ice} \cdot T_{ice}}{\Delta t} & \textit{if } \Delta M_F > 0 \end{cases} \tag{14}$$

with c_{ice} as the specific heat of ice.

1.2.5 Bulk Icestupa heat flux q_G

The bulk Icestupa heat flux q_G corresponds to the ground heat flux in normal soils and is caused by the temperature gradient between the surface layer (T_{ice}) and the ice body (T_{bulk}). It is expressed by using the heat conduction equation as follows:

$$q_G = k_{ice} \cdot (T_{bulk} - T_{ice})/l_{ice} \tag{15}$$

where k_{ice} is the thermal conductivity of ice (2.123 $W\,m^{-1}\,K^{-1}$) , T_{bulk} is the mean temperature of the ice body within the Icestupa and l_{ice} is the average distance of any point in the surface to any other point in the ice body. T_{bulk} is initialised as 0 $^{\circ}C$ and later determined from Eqn. 15 as follows:

$$T_{bulk}^{i+1} = T_{bulk} - (q_G \cdot A \cdot \Delta t)/(M_{ice} \cdot c_{ice}) \tag{16}$$

Since we assume a conical shape with $r_{ice} > h_{ice}$, l_{ice} cannot be greater than $2r_{ice}$ and also cannot be less than Δx. Therefore, the average distance from any point on the surface to any point inside is $\Delta x \leq l_{ice} \leq r_{ice}$. We calculate q_G here assuming $l_{ice} = r_{ice}/2$.

1.3 Surface temperature and phase change processes

The available energy q_{surf} can act on the surface of the AIR to a) change its temperature, b) melt ice or c) freeze ice. So Eqn. 6 can be rewritten as:

$$q_{surf} = q_{freeze/melt} + q_T \tag{17}$$

where q_T, q_{freeze} and q_{melt} represent energy associated with process (a), (b) and (c) respectively.

To distribute the surface energy flux into these three components, we categorize the model time steps as freezing or melting events. Freezing events can only occur if there is fountain water available and the surface energy flux is negative. But just these two conditions are not sufficient as the latent heat energy can only contribute to temperature fluctuations.

$$q_{freeze/melt} = \begin{cases} q_{freeze} & \textit{if } \Delta M_F > 0 \textit{ and } q_{surf} < 0 \textit{ and } (q_{surf} - q_L) < 0 \\ q_{melt} & \textit{otherwise} \end{cases} \tag{18}$$

During a freezing event, the available energy $(q_{surf} - q_L)$ can either be sufficient or insufficient to freeze the fountain water available. If insufficient, the additional energy further cools down the surface temperature. So the surface energy flux distribution during a freezing event can be represented as:

$$(q_{freeze}, q_T) = \begin{cases} (q_{surf} - q_L, q_L) & \textit{if } \Delta M_F \geq -\frac{(q_{surf} - q_L) A \cdot \Delta t}{L_f} \\ (\frac{\Delta M_F \cdot L_f}{A \cdot \Delta t}, q_{surf} + \frac{\Delta M_F \cdot L_f}{A \cdot \Delta t}) & \textit{if } \Delta M_F < -\frac{(q_{surf} - q_L) A \cdot \Delta t}{L_f} \end{cases} \tag{19}$$

Table 1. Free parameters in the model categorised as constant, uncertain and site parameters. Base value (B) and uncertainty (U) were taken from the literature. For assumptions (assum.), the uncertainty was chosen to be relatively large (5 %). For measurements (meas.), the uncertainty due to parallax errors is chosen to be (1 %).

Constant Parameters	Symbol	Value		References
Van Karman constant	κ	0.4		B: Cuffey and Paterson
Stefan Boltzmann constant	σ	$5.67 \cdot 10^{-8} W\, m^{-2}\, K^{-4}$		B: Cuffey and Paterson
Air pressure at sea level	$p_{0,a}$	1013 hPa		B: Mölg and Hardy
Density of water	ρ_w	1000 $kg\, m^{-3}$		B: Cuffey and Paterson
Density of ice	ρ_{ice}	917 $kg\, m^{-3}$		B: Cuffey and Paterson
Density of air	ρ_a	1.29 $kg\, m^{-3}$		B: Mölg and Hardy
Specific heat of ice	c_{ice}	2097 $J\, kg^{-1}\, °C^{-1}$		B: Cuffey and Paterson
Specific heat of water	c_w	4186 $J\, kg^{-1}\, °C^{-1}$		B: Cuffey and Paterson
Specific heat of air	c_a	1010 $J\, kg^{-1}\, °C^{-1}$		B: Mölg and Hardy
Thermal conductivity of ice	k_{ice}	2.123 $W\, m^{-1}\, K^{-1}$		B: Bonales et al.
Latent Heat of Sublimation	L_s	2848 $kJ\, kg^{-1}$		B: Cuffey and Paterson
Latent Heat of Fusion	L_f	334 $kJ\, kg^{-1}$		B: Cuffey and Paterson
Uncertain Parameters			**Range**	
Precipitation Temperature threshold	T_{ppt}	1 °C	$\pm\, 1\, °C$	B + U: Fujita and Ageta, Zhou et al.
Ice Emissivity	ϵ_{ice}	0.95	[0.949,0.993]	B: Cuffey and Paterson; U: Hori et al.
Ice Albedo	α_{ice}	0.35	$\pm$ 5 %	B: Cuffey and Paterson; U: assum.
Snow Albedo	α_{snow}	0.85	$\pm$ 5 %	B: Cuffey and Paterson; U: assum.
Albedo Decay Rate	τ	10 days	$[1, 22]\, days$	B: Schmidt et al.; U: Oerlemans and Knap
Surface layer thickness	Δx	20 mm	$[1, 10]\, mm$	assum.

During a melting event, the surface energy flux (q_{surf}) is first used to change the surface temperature to T_{temp} calculated as:

$$T_{temp} = \frac{q_{surf} \cdot \Delta t}{\rho_{ice} \cdot c_{ice} \cdot \Delta x} + T_{ice} \tag{20}$$

If $T_{temp} > 0°C$, then energy is reallocated from q_T to q_{melt} and produce meltwater. So the surface energy flux distribution during a melting event can be represented as:

$$(q_{melt}, q_T) = \begin{cases} (0, q_{surf}) & if\, T_{temp} < 0 \\ (\frac{T_{temp} \cdot \rho_{ice} \cdot c_{ice} \cdot \Delta x}{\Delta t}, q_{surf} - \frac{T_{temp} \cdot \rho_{ice} \cdot c_{ice} \cdot \Delta x}{\Delta t}) & if\, T_{temp} > 0 \end{cases} \tag{21}$$

1.4 Mass Balance

The mass balance equation is used to derive the water that drains away (M_{runoff}) as follows:

$$\frac{\Delta M_F + \Delta M_{ppt} + \Delta M_{dep}}{\Delta t} = \frac{\Delta M_{ice} + \Delta M_{water} + \Delta M_{sub} + \Delta M_{runoff}}{\Delta t} \tag{22}$$

$$\frac{\Delta M_{ppt}}{\Delta t} = \begin{cases} \pi \cdot {r_{ice}}^2 \cdot \rho_w \cdot ppt & if\, T_a < T_{ppt} \\ 0 & if\, T_a \geq T_{ppt} \end{cases} \tag{23a}$$

$$(\frac{\Delta M_{dep}}{\Delta t}, \frac{\Delta M_{sub}}{\Delta t}) = \begin{cases} \frac{q_L \cdot A}{L_s} \cdot (1, 0) & if\, q_L \geq 0 \\ \frac{q_L \cdot A}{L_s} \cdot (0, -1) & if\, q_L < 0 \end{cases} \tag{23b}$$

$$\frac{\Delta M_{water}}{\Delta t} = \frac{q_{melt} \cdot A}{L_f} \tag{23c}$$

$$\frac{\Delta M_{ice}}{\Delta t} = \frac{q_{freeze} \cdot A}{L_f} + \frac{\Delta M_{ppt}}{\Delta t} + \frac{\Delta M_{dep}}{\Delta t} - \frac{\Delta M_{sub}}{\Delta t} - \frac{\Delta M_{melt}}{\Delta t} \tag{23d}$$

$$\frac{\Delta M_{runoff}}{\Delta t} = \frac{\Delta M_F - \Delta M_{ice}}{\Delta t} \tag{23e}$$

REFERENCES

Bonales, L. J., Rodriguez, A. C., and Sanz, P. D. (2017). Thermal conductivity of ice prepared under different conditions. *International Journal of Food Properties* 20, 610–619. doi:10.1080/10942912.2017.1306551

Cuffey, K. M. and Paterson, W. S. B. (2010). *The Physics Of Glaciers* (Elsevier)

Fujita, K. and Ageta, Y. (2000). Effect of summer accumulation on glacier mass balance on the tibetan plateau revealed by mass-balance model. *Journal of Glaciology* 46, 244–252. doi:10.3189/172756500781832945

Garratt, J. R. (1992). *The Atmospheric Boundary Layer* (Cambridge University Press)

Hock, R. (2005). Glacier melt: a review of processes and their modelling. *Progress in Physical Geography: Earth and Environment* 29, 362–391

Hori, M., Aoki, T., Tanikawa, T., Motoyoshi, H., Hachikubo, A., Sugiura, K., et al. (2006). In-situ measured spectral directional emissivity of snow and ice in the 8–14 micrometer atmospheric window. *Remote Sensing of Environment* 100, 486 – 502

Mölg, T. and Hardy, D. R. (2004). Ablation and associated energy balance of a horizontal glacier surface on kilimanjaro. *J. Geophys. Res.-Atmos.* 109, 1–13. doi:10.1029/2003JD004338

Oerlemans, J. and Knap, W. H. (1998). A 1 year record of global radiation and albedo in the ablation zone of morteratschgletscher, switzerland. *Journal of Glaciology* 44, 231–238. doi:10.3189/S0022143000002574

Schmidt, L. S., Aðalgeirsdóttir, G., Guðmundsson, S., Langen, P. L., Pálsson, F., Mottram, R., et al. (2017). The importance of accurate glacier albedo for estimates of surface mass balance on vatnajökull: evaluating the surface energy budget in a regional climate model with automatic weather station observations. *The Cryosphere* 11, 1665–1684. doi:10.5194/tc-11-1665-2017

WMO (2018). *Guide to Instruments and Methods of Observation* (World Meteorological Organization ; 2018 (2018 Edition))

Woolf, H. M. (1968). *On the Computation of Solar Elevation Angles and the determination of sunrise and sunset times* (National Aeronautics and Space Administration)

Zhou, S., Kang, S., Gao, T., and Zhang, G. (2010). Response of zhadang glacier runoff in nam co basin, tibet, to changes in air temperature and precipitation form. *Chinese Science Bulletin* 55, 2103–2110. doi:10.1007/s11434-010-3290-5